

HASACL-~~7354~~  
-73514

NATIONAL AERONAUTICS AND SPACE ADMINISTRATION

*Technical Report 32-1314*

*Digital Demodulation with Data Subcarrier Tracking*

*David K. Sanger*

JET PROPULSION LABORATORY  
CALIFORNIA INSTITUTE OF TECHNOLOGY  
PASADENA, CALIFORNIA

August 1, 1968

NATIONAL AERONAUTICS AND SPACE ADMINISTRATION

*Technical Report 32-1314*

*Digital Demodulation with Data Subcarrier Tracking*

*David K. Sanger*

JET PROPULSION LABORATORY  
CALIFORNIA INSTITUTE OF TECHNOLOGY  
PASADENA, CALIFORNIA

August 1, 1968

**TECHNICAL REPORT 32-1314**

Copyright © 1969  
Jet Propulsion Laboratory  
California Institute of Technology

Prepared Under Contract No. NAS 7-100  
National Aeronautics and Space Administration

## **Preface**

The work described in this report was performed by the Telecommunications Division of the Jet Propulsion Laboratory.



## Contents

<b>I. Introduction</b> . . . . .	1
<b>II. Analysis of the Theoretical Model</b> . . . . .	1
A. Development of the Model . . . . .	1
B. System Description . . . . .	2
C. Subcarrier Tracking Loop . . . . .	3
D. Bit Timing Loop . . . . .	7
E. Digitization . . . . .	12
F. Probability of Error . . . . .	12
<b>III. Software Description</b> . . . . .	13
A. The Computer and ADC . . . . .	13
B. The Subcarrier Tracking Loop . . . . .	13
C. Bit Timing Loop . . . . .	13
D. Frame Sync and Word Sync . . . . .	13
E. Computer Scaling . . . . .	15
F. Variable Loop Parameters . . . . .	15
<b>IV. System Design</b> . . . . .	15
A. Subcarrier Tracking Loop . . . . .	15
B. Bit Timing Loop . . . . .	15
C. Performance . . . . .	15
<b>V. Summary and Recommendations</b> . . . . .	16
A. Square Wave VCO Output Waveform . . . . .	16
B. T/3 Bit Timing . . . . .	16
C. The Difference of Absolute Values . . . . .	16
D. Storage of the Error Voltages for Four Bit Times . . . . .	16
<b>References</b> . . . . .	17

## Figures

1. Mariner two-channel subcarrier telemetry spectrum . . . . .	2
2. Ground receiver and digital demodulator system . . . . .	2
3. Amplifier gain characteristic curve . . . . .	3

## Contents (contd)

### Figures (contd)

4. Demodulator functional diagram . . . . .	3
5. Subcarrier tracking loop: integrator output showing the effect of bit timing error . . . . .	5
6. Subcarrier tracking loop: standard deviation of the phase error . . . . .	7
7. Bit timing loop: integrator output showing the effect of bit timing error . . . . .	9
8. Bit timing loop: average bit timing loop error voltage. . . . .	11
9. Mean output of a digital voltage controlled oscillator . . . . .	12
10. Computer algorithm for the subcarrier tracking loop . . . . .	14
11. Computer algorithm for the bit timing loop . . . . .	14
12. Digital demodulator error probability . . . . .	16

## **Abstract**

The concept of digital telemetry demodulation depends upon a computer algorithm to accomplish bit synchronization by testing the incoming data stream over intervals that are one-third of a bit time early and one-third of a bit time late with respect to the estimated data transition time. Correct bit synchronization results when the estimated timing intervals have been adjusted properly. This early-late bit timing scheme coupled with a Costas data tracking loop is the basis for the digital demodulator discussed in this report.





# Digital Demodulation with Data Subcarrier Tracking

## I. Introduction

During the months of August and September, 1967, the earth, *Mariner IV*, and *Mariner V* were in relative positions to measure the effect of certain solar particles that follow spiral and linear paths as they travel outward from the sun. This was an exciting possibility when it is considered that this was the first time such a situation had occurred with these spacecraft. An analysis of the Deep Space Network (DSN) tracking capability during this period showed that with both spacecraft operating on their omnidirectional antennas and while being tracked with the 85-ft-diam DSN antenna, there was sufficient received signal strength to maintain lock on the RF carrier. However, using the standard *Mariner C* two-channel telemetry demodulator (Ref. 1), the bit error rate at this low signal level would be excessive because of the difficulty in maintaining demodulator lock in the telemetry sync channel. Thus, an effort was undertaken to develop a digital data subcarrier demodulator. This effort was constrained to demodulate the *Mariner IV* and *Mariner V* 8½-bit/s telemetry in the spacecraft data mode II. In addition, it would interface directly with the decommutation program presently in use at the DSN stations for the *Mariner V* mission.

This report is intended to analyze the technique, describe the operation, and present some of the results obtained while the demodulator was used by the *Mariner IV* and *V* spacecraft.

## II. Analysis of the Theoretical Model

### A. Development of the Model

The *Mariner IV* and *V* communication system is a binary phase-shifted-keyed (PSK) two-channel telemetry system. In a two-channel system (Ref. 2), one channel conveys synchronization information (bit-sync and subcarrier phase information) and the other channel transmits the data. There is no overlap in the frequency spectrum, since the sync subcarrier is at the frequency  $2f_s$  and the data subcarrier channel is at the frequency  $4f_s$ . To coherently demodulate either subcarrier, it is necessary to estimate the phase and frequency of the subcarrier.

The *Mariner C* hardware demodulator utilizes both of these channels for telemetry demodulation. At low signal levels, however, the bit error rate is high because of the inability to maintain lock on the sync channel. The power contained in this sync channel, however, does not convey any information other than the phase and frequency of the subcarrier and bit sync information, which can be derived from the data subcarrier.

A number of methods have been proposed for generating the phase and frequency reference from the received data subcarrier, thus eliminating the need for a separate sync subcarrier, even in the absence of a dc component in the modulation. The first method, the squaring loop,

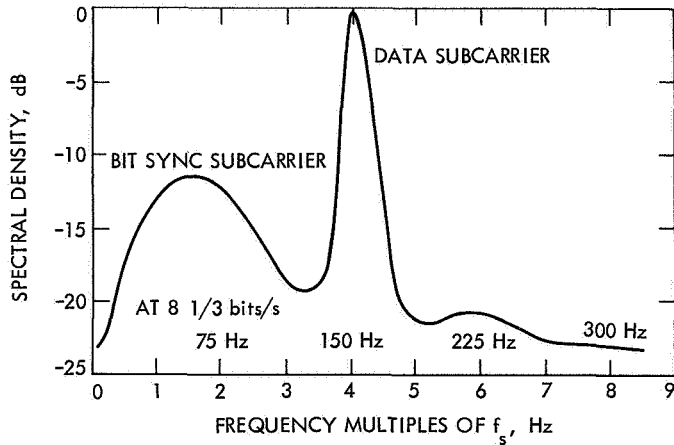


**Fig. 1. Mariner two-channel subcarrier telemetry spectrum**

has been analyzed in several papers (Refs. 3-5). A second method, originally proposed by Costas (Ref. 6) has been analyzed by Stiffler (Ref. 7) and Lindsey (Ref. 8) and was shown to be equivalent, theoretically, to the squaring loop.

Based on this theory, if the output of the carrier tracking loop in the receiver is passed through a bandpass filter centered on the  $4f_s$  data subcarrier (Fig. 1), then the input to the digital demodulator is the binary PSK data subcarrier signal  $y(t)$ . This filter reduces the noise and eliminates the sync subcarrier and all harmonics of the square wave data channel. The phase and the frequency information can then be derived from the data signal using the Costas loop technique.

Bit timing can be achieved through an early-late timing scheme. Optimum bit timing estimation, however, requires the testing of each possible bit time and forming the product of the hyperbolic cosines of the matched filter outputs (Ref. 9). The optimum estimate corresponds

to the largest product. This procedure would require a very fast computer to operate in real time. An alternative is to approximate the hyperbolic cosine by a parabola, which is valid for low signal-to-noise ratios, and thus only compute the sums of squares. A second alternative, and one that is quite practical to realize, is to test only early and late timing instead of testing every possible time. This early-late bit timing scheme coupled with the Costas subcarrier tracking loop is the basis for providing the necessary timing information required to demodulate the data.

### B. System Description

The receiver-demodulator system diagram is shown in Fig. 2. The tracking receiver output, after passing through the bandpass filter, centered on the  $4f_s$  data subcarrier is the data subcarrier  $y(t)$

$$y(t) = \sqrt{2} A m(t) \cos(\omega t + \theta) + n(t) \quad (1)$$

for the binary signal,  $m(t) = \pm 1$ . Equation (1) can then be rewritten as

$$y(t) = \sqrt{2} A \sin(\omega t + \theta + m) + n(t) \quad (2)$$

where

$\theta$  = phase of the received subcarrier

$\omega$  = frequency of the received data subcarrier =  $4f_s$

$m = \pm \pi/2$

$n(t)$  = white gaussian noise with zero mean, and one-sided spectral density,  $N_0$  w/Hz

$A$  = data channel rms voltage

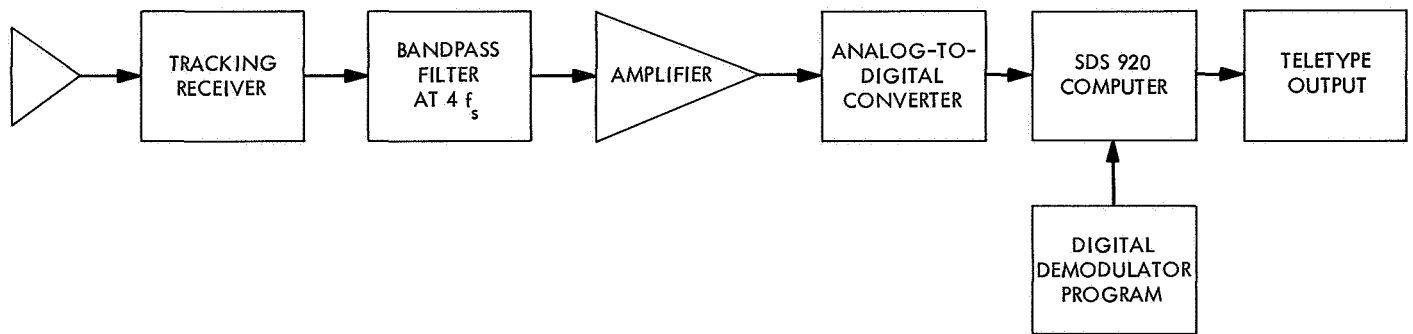


**Fig. 2. Ground receiver and digital demodulator system**

The output of the bandpass filter is capacitively coupled to an amplifier that limits the input to the analog-to-digital converter (ADC). The ADC input voltage is a variable function of the amplifier input signal-to-noise ratio per bit ( $ST/N_0$ ) as shown in Fig. 3. The amplifier has an AGC loop on the noise such that the signal input voltage to the ADC is constant at 0.96V rms. It will be shown later in this report that the bit timing loop and subcarrier phase loop threshold constants are both functions of the input signal amplitude. Use of the AGC loop in the amplifier allows the selection of the loop constants for use with varying  $ST/N_0$ .

This telemetry demodulator is designed to operate on the standard Deep Space Network (DSN) computer: the Scientific Data Systems (SDS) 920. This computer has a relatively slow computation time and its speed is an important factor when deciding which operations can be performed between ADC samples.

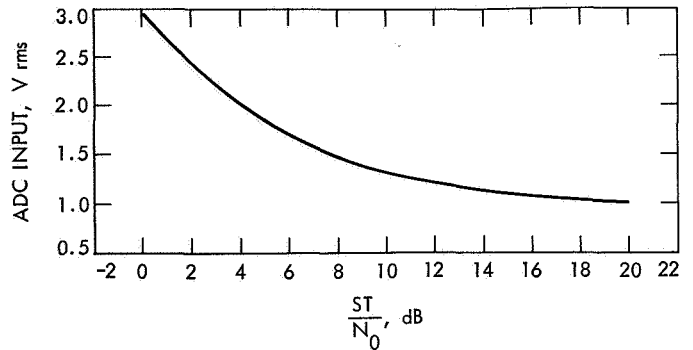


Fig. 3. Amplifier gain characteristic curve

### C. Subcarrier Tracking Loop

The digital demodulator block diagram is shown in Fig. 4. The lower section, which is the subcarrier tracking loop, is a standard Costas loop. The phase of the data

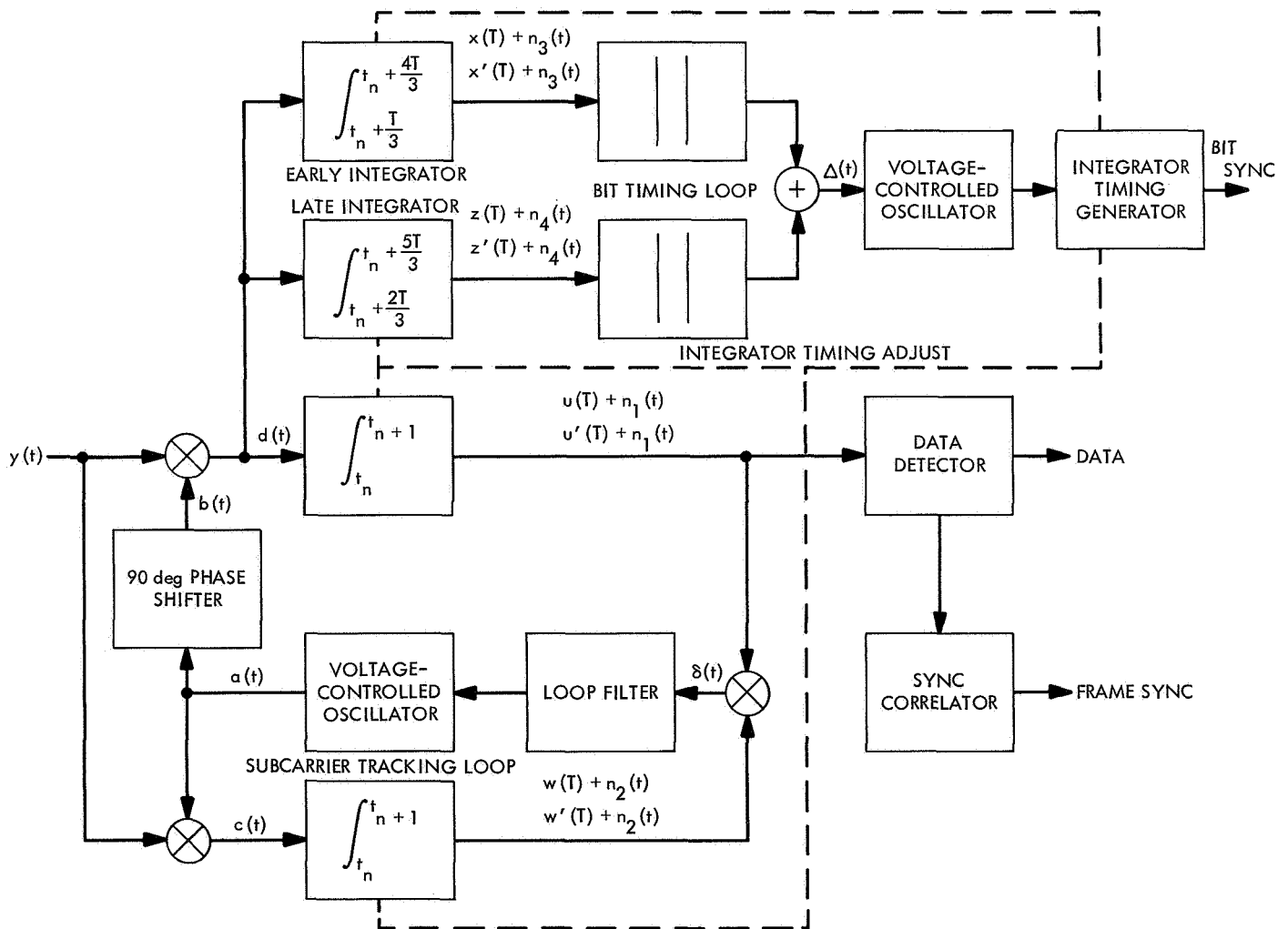


Fig. 4. Demodulator functional diagram

subcarrier is extracted from the suppressed carrier signal plus noise  $y(t)$  by multiplying the input voltage of the two integrators (equivalent low-pass filters) with that produced from the square wave output of the digital voltage controlled oscillator (VCO) and a 90-deg phase shift of that voltage. The integrator outputs are then multiplied, and this signal is used to control the phase of the loop VCO. If  $\theta$  is the phase of the incoming signal and  $\hat{\theta}$  is the phase of the loop VCO, then the Costas loop will attempt to zero the loop phase error,  $\phi = \theta - \hat{\theta}$ .

This analysis will assume that the loop phase error is constant over the duration of the bit time. Also, a bar over a variable will be used to indicate the ensemble average. The loop VCO output is a square wave whose Fourier series expansion is

$$a(t) = \sum_{n=1}^{\infty} \frac{2}{n\pi} (1 - \cos n\pi) \sin(n\omega t + \hat{\theta}) \quad (3)$$

After passing  $a(t)$  through the 90-deg phase shifter, we have a similar Fourier series for  $b(t)$ :

$$b(t) = \sum_{n=1}^{\infty} \frac{4}{n\pi} \left[ \sin\left(\frac{n\pi}{2}\right) \cos(n\omega t + \hat{\theta}) \right] \quad (4)$$

The output of the lower multiplier  $c(t)$  consists of the input signal plus noise multiplied by the VCO square wave.

$$c(t) = y(t) \cdot a(t) + n(t) \cdot a(t) \quad (5)$$

After multiplying and using the trigonometric identity,

$$2 \sin(A) \sin(B) = \cos(A - B) - \cos(A + B) \quad (6)$$

and realizing that the integrator acts like a low-pass filter (passing only the fundamental terms),

$$c(t) = \pm \frac{2\sqrt{2}}{\pi} A \sin(\phi) + a(t) \cdot n(t) \quad (7)$$

likewise, the output of the upper integrator is

$$d(t) = \pm \frac{2\sqrt{2}}{\pi} A \cos(\phi) + b(t) \cdot n(t) \quad (8)$$

Digress for a moment to consider the effect of multiplying white Gaussian noise (Ref. 10) by the VCO output

square wave and the effect of the low-pass filter (integrator). Define

$$n_1(t) = \left[ \frac{4}{\pi} n(t) \cos(\omega t) \right]_{LF} = \frac{2}{\pi} n_{\beta}(t) \quad (9)$$

$$n_2(t) = \left[ \frac{4}{\pi} n(t) \sin(\omega t) \right]_{LF} = \frac{2}{\pi} n_{\alpha}(t) \quad (10)$$

where  $n(t) = n_{\alpha}(t) \cos(\omega t + \theta) + n_{\beta}(t) \sin(\omega t + \theta)$  and  $n_{\alpha}(t)$  and  $n_{\beta}(t)$  are stationary independent sample functions of a stationary random process. Thus,  $n_1(t)$  and  $n_2(t)$  are independent since  $n_{\alpha}(t)$  and  $n_{\beta}(t)$  are statistically independent. (The subscripts *LF* indicate that only the low-frequency components are retained.) The mean and variance are

$$\left. \begin{aligned} \overline{n_1(t)} = \overline{n_2(t)} &= 0 \\ \sigma_{n_1}^2 = \sigma_{n_2}^2 &= \sigma_n^2 \end{aligned} \right\} \quad (11)$$

where  $\sigma_n^2$  is the variance of the noise after passage through the integrator.

The integral of white gaussian noise is the well-documented Wiener-Levy process (Ref. 11). If the input noise process has one-sided spectral density  $N_0$  V<sup>2</sup>/Hz (or two-sided density  $N_0/2$  V<sup>2</sup>/Hz), then the variance,  $\sigma_n^2$  of the integrated gaussian density is

$$\sigma_n^2 = \frac{N_0 T}{2} \quad (12)$$

This concludes this short digression on the noise.

Next, look at the passage of signal through the two integrators, considering first the upper integrator and then the lower integrator. For the upper integrator,

$$u(T) = \int_{t_n}^{t_{n+1}} d(t) dt \quad (13)$$

and for the lower integrator,

$$w(T) = \int_{t_n}^{t_{n+1}} c(t) dt \quad (14)$$

Before considering the integration process directly, the effects of the timing error  $\tau$  and data transitions must be investigated. The time difference between the start of a

bit and the start of the integration will be referred to as a bit timing error  $\tau$ . The function of the bit timing loop (to be discussed in the next section) is to adjust the integrator start time so  $\tau = 0$  and thus the integration is over one bit time. A bit transition is then coincident with the beginning and the end of each integration time. Let a prime (') denote a data transition (-1 to +1 or +1 to -1) and no prime denote no transition between two adjacent bit times.

For the no-transition case,

$$u(T) = \frac{2\sqrt{2}AT}{\pi} \cos(\phi) \quad (15)$$

$$w(T) = \frac{2\sqrt{2}AT}{\pi} \sin(\phi) \quad (16)$$

Figure 5 shows the four possible transition cases. The integrals (Eqs. 13 and 14) can be computed for the four possible cases. In summary:

$$u'(T) = \pm \frac{2\sqrt{2}A}{\pi} (T - 2|\tau|) \cos(\phi) \quad (17)$$

$$w'(T) = \pm \frac{2\sqrt{2}A}{\pi} (T - 2|\tau|) \sin(\phi) \quad (18)$$

The VCO control voltage  $\delta(t)$  becomes

$$\delta(t) = [u(T) + n_1(t)] [w(T) + n_2(t)] \quad (19)$$

When  $\delta(t)$  is averaged over the probability spaces of the noise and transitions, recall:

- (1) Probability of a transition = probability of no transition = 1/2.
- (2) The two noise functions are mutually independent.
- (3) The signal and noise are mutually independent.

If we assume that  $\phi$  and  $\tau$  are slowly varying functions of time, then the average loop phase error  $\bar{\delta}$  will only be a random function of the transition probability.

Define

$$\bar{\delta(t)} = \frac{1}{2} \overline{\delta'(t)} + \frac{1}{2} \overline{\delta(t)} \quad (20)$$

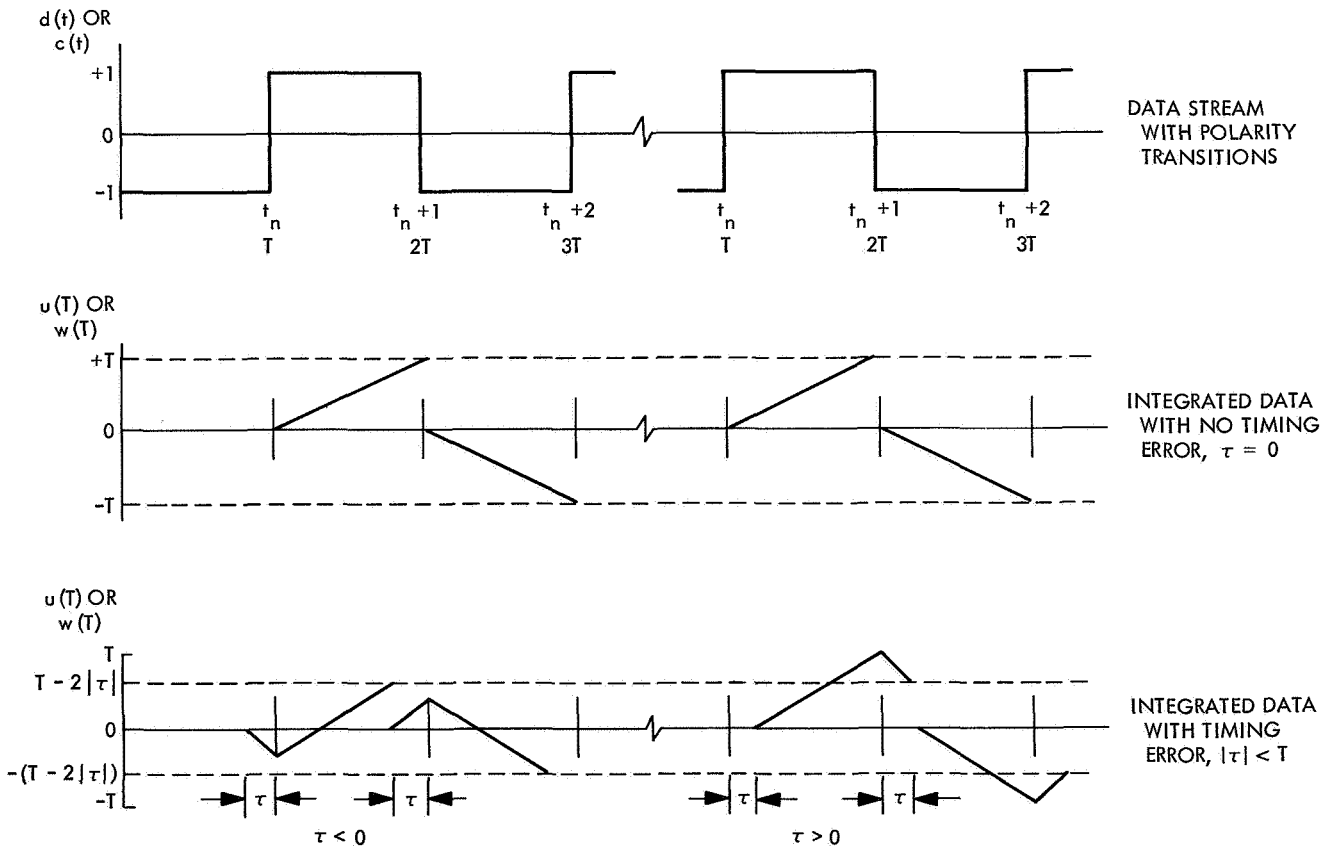


Fig. 5. Subcarrier tracking loop: integrator output showing the effect of bit timing error

Then,

$$\overline{\delta(t)} = \frac{2A^2}{\pi^2} [T^2 + (T - 2|\tau|)^2] \sin(2\phi) \quad (21)$$

The variance of  $\delta$ , given that  $\tau$  and  $\phi$  are constant over a bit duration will be needed to formulate the subcarrier phase jitter  $\sigma_\phi$ . Since

$$\sigma_\delta^2 = \overline{\delta^2(t)} - \overline{\delta(t)}^2 \quad (22)$$

after squaring  $\delta(t)$  and averaging over the transition and noise probabilities, we have

$$\begin{aligned} \overline{\delta^2(t)} &= \frac{16A^4}{\pi^4} [T^2 + (T - 2|\tau|)^2] \sin^2(2\phi) \cos^2(2\phi) \\ &+ \frac{A^2 N_0 T}{\pi^2} [T^2 + (T - 2|\tau|)^2] + \frac{N_0^2 T^2}{4} \end{aligned} \quad (23)$$

and

$$\sigma_\delta^2 = \frac{A^2 N_0 T}{\pi^2} [T^2 + (T - 2|\tau|)^2] + \frac{N_0^2 T^2}{4} \quad (24)$$

A computed value of  $\delta$  at some time  $t$  (where  $t$  is an integer number at bit periods) has some error,  $E$ , due to the noise.

$$\delta(t) = \overline{\delta(t)} + E_t \quad (25)$$

If it is assumed that  $\phi$  is small and that the linear assumption holds,  $\sin(2\phi) \approx 2\phi$

$$\delta(t) = h\phi + E_t \quad (26)$$

where

$$h = \frac{4A^2}{\pi^2} [T^2 + (T - 2|\tau|)^2]$$

The subcarrier tracking loop is closed by changing the estimated phase  $\phi$  according to the measured error signal  $\delta(t)$

$$\phi_{t+1} = \phi_t - K_o K_m F(p) \delta(t) \quad (27)$$

where

$K_o$  = VCO gain constant

$K_m$  = multiplier constant

$F(p)$  = loop filter transfer function

If we let  $c = K_o K_m$  and consider a first-order phase-locked loop, i.e.,  $F(p) = 1$ ,

$$\phi_{t+1} = \phi_t - c\delta(t) \quad (28)$$

in the absence of noise,

$$\phi_t = (1 - ch)^n \phi_0 \quad (29)$$

where

$\phi_0$  = the initial subcarrier tracking loop phase error

$n = t/T$

Equations (26) and (29) combine to yield an expression for the variance of the tracking loop phase error,  $\sigma_\phi^2$ :

$$\begin{aligned} \sigma_\phi^2 &= \frac{ch}{2 - ch} \left( \frac{\sigma_\delta^2}{h^2} \right) \\ &= \frac{ch}{2 - ch} \left( \frac{N_0 T \pi^2}{8A^2 [T^2 + (T - 2|\tau|)^2]} \right. \\ &\quad \left. + \left\{ \frac{N_0 T \pi^2}{8A^2 [T^2 + (T - 2|\tau|)^2]} \right\}^2 \right) \end{aligned} \quad (30)$$

when the bit timing loop is locked,  $\tau = 0$ , and

$$\sigma_\phi^2 = \frac{ch}{2 - ch} \left[ \left( \frac{N_0 \pi^2}{16A^2 T} \right) + \left( \frac{N_0 \pi^2}{16A^2 T} \right)^2 \right] \quad (31)$$

If the output of the VCO is not a square wave with fundamental amplitude  $4/\pi$  but is a sine wave with peak amplitude  $\sqrt{2}$ , then the variance of the phase error is

$$\sigma^2 = \frac{ch}{2 - ch} \left[ \left( \frac{N_0}{2A^2 T} \right) + \left( \frac{N_0}{2A^2 T} \right)^2 \right] \quad (32)$$

Figure 6 shows the 0.9-dB degradation in performance when the sine wave subcarrier is demodulated with a square wave VCO output waveform (Eqs. 31 and 32).

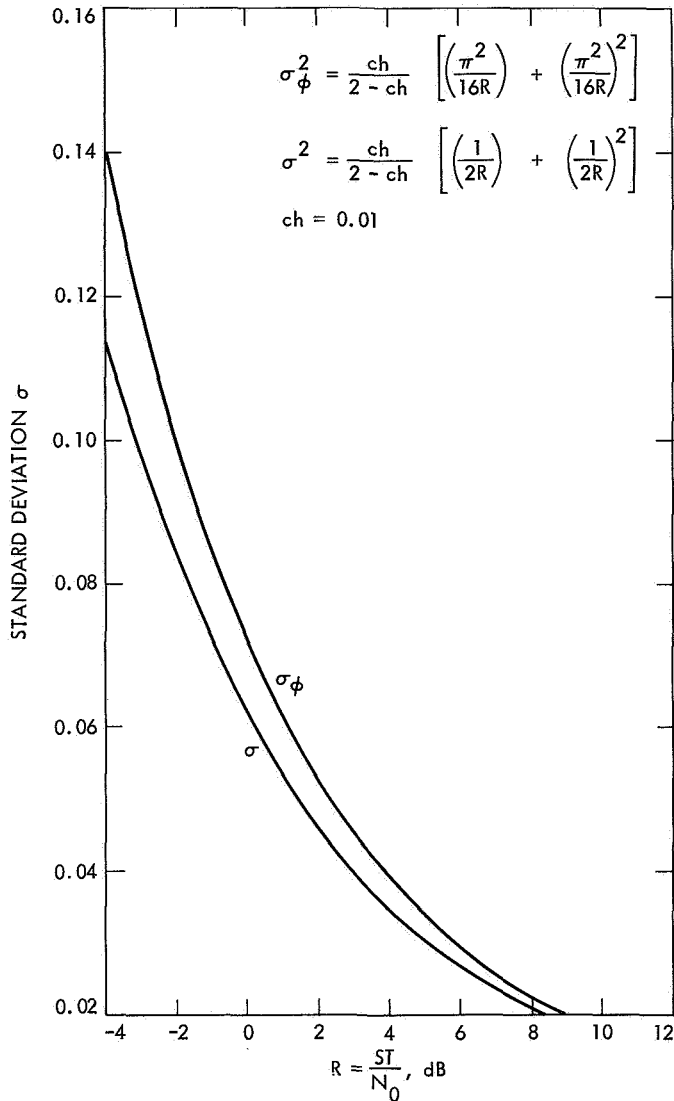


**Fig. 6. Subcarrier tracking loop: standard deviation of the phase error**

#### D. Bit Timing Loop

As discussed in the preceding section, the occurrence of a data polarity transition and the bit duration must be known before the data can be processed. The digital demodulator accomplishes bit timing by integrating  $d(t)$  over a bit duration that begins at one-third of a bit time before the local estimate of a bit transition. Independently,  $d(t)$  is also integrated one-third of a bit time after the local estimate. When these two integrator outputs are differenced in absolute value, the difference, or error signal,  $\Delta(t)$ , will be zero if there is no error in the local estimate. If  $\Delta(t)$  is not zero, the local estimate of a bit transition time is incremented and the integration start and dump time in the bit timing loop and subcarrier

tracking loop ( $\tau$  contributes to  $\sigma_{\phi}^2$  in Eq. 30) is adjusted to produce a new  $\Delta(t)$ .

Consider first the integration of the signal portion of  $d(t)$  in the early timing integrator for no data transitions between sample periods. The signal output of the early integrator  $x(T)$

$$x(T) = \int_{t_n + T/3}^{t_{n+1} + T/3} d(t) dt = \pm \frac{2\sqrt{2}AT \cos(\phi)}{\pi} \quad (33)$$

and likewise for the late integrator

$$z(T) = \int_{t_n + 2T/3}^{t_{n+1} + 2T/3} d(t) dt = \pm \frac{2\sqrt{2}AT \cos(\phi)}{\pi} \quad (34)$$

Considering now the noise, let the noise output of the early and late integrators be  $n_3(t)$  and  $n_4(t)$ , respectively. The mean and variance of  $n_3(t)$  and  $n_4(t)$  are the same as for  $n_1(t)$ .

$$\overline{n_3(t)} = \overline{n_4(t)} = 0 \quad (35)$$

$$\overline{n_3^2(t)} = \overline{n_4^2(t)} = \sigma_n^2 = \frac{N_0 T}{2} \quad (36)$$

As in the subcarrier tracking loop, the effect of data transitions must be considered. The early and late integrator signal output for transitions with bit timing error  $\tau$  is shown in Fig. 7: After integrating  $d(t)$  and considering an error  $\tau$  in the local integrator output for the data estimate, we have for the signal:

$$x'(T) = \pm \frac{2\sqrt{2}A}{\pi} \left( \frac{T}{3} - 2\tau \right) \cos(\phi) \quad \tau \leq \frac{T}{6} \quad (37)$$

For the late integrator the output for a data transition is

$$z'(T) = \pm \frac{2\sqrt{2}A}{\pi} \left( \frac{T}{3} + 2\tau \right) \cos(\phi) \quad \tau \leq \frac{T}{6} \quad (38)$$

The noise terms  $n_3(t)$  and  $n_4(t)$  are defined in Eqs. (35) and (36).



After taking the absolute value of the integrator output and differencing, we have the bit timing loop error voltage,  $\Delta(t)$ .

$$\Delta(t) = \begin{cases} |z(T) + n_4(t)| - |x(T) + n_3(t)| & \text{with probability} = \frac{1}{2} \\ |z'(T) + n_4(T)| - |x'(T) + n_3(t)| & \text{with probability} = \frac{1}{2} \end{cases} \quad (39)$$

The noise is gaussian with zero mean and the "signal"—i.e.,  $z(T)$  or  $x(T)$ —is constant over a bit time. Thus,  $[z(T) + n_4(t)]$  and  $[x(T) + n_3(t)]$  can be considered gaussian random processes with mean equal to the "signal,"  $z(T)$  or  $x(T)$ . The statistics of  $\Delta(t)$  are then independent functions of the equiprobable transition occurrence and this nonzero mean gaussian process.

Next, we investigate the mean bit timing error,  $\overline{\Delta(t)}$ . By definition:

$$\Delta(t) = \frac{1}{2} [ |z(T) + n_4(t)| - |x(T) + n_3(t)| + |z'(T) + n_4(t)| - |x'(T) + n_3(t)| ] \quad (40)$$

Consider a general case for the nonzero gaussian process. Let

$$y(t) = \lambda + n(t) \quad (41)$$

where  $y(t)$  is a gaussian random variable with mean  $\lambda$  and variance  $\sigma^2$ .

Therefore,

$$p(y) = \frac{1}{\sqrt{2\pi}\sigma} \exp \left[ -\frac{(y-\lambda)^2}{2\sigma^2} \right] \quad (42)$$

Then,

$$\begin{aligned} |\overline{y(T)}| &= \int_{-\infty}^{\infty} |y| p(y) dy \\ &= \frac{\sigma}{\sqrt{2\pi}} \int_{\left(\frac{\lambda}{\sigma}\right)^2}^{\infty} e^{-\frac{x}{2}} dx + \frac{2\lambda}{\sqrt{2\pi}} \int_0^{\left(\frac{\lambda}{\sigma}\right)^2} e^{-\frac{x}{2}} dx \end{aligned} \quad (43)$$

$$\quad (44)$$

But the second integral is the error function

$$\text{erf}(v) = \frac{1}{\sqrt{2\pi}} \int_0^v e^{-\frac{x^2}{2}} dx \quad (45)$$

and then we have

$$|\overline{y(T)}| = \frac{2\sigma}{\sqrt{2\pi}} \exp \left[ -\frac{1}{2} \left( \frac{\lambda}{\sigma} \right)^2 \right] + 2\lambda \text{erf} \left( \frac{\lambda}{\sigma} \right) \quad (46)$$

Equation (40) can now be solved for  $\Delta(t)$  using the results given in Eq. (46).

$$\begin{aligned} \overline{\Delta(t)} &= \frac{1}{2} \sqrt{\frac{N_0 T}{\pi}} \left( \exp \left\{ \frac{-[z'(T)]^2}{N_0 T} \right\} \right. \\ &\quad \left. - \exp \left\{ \frac{-[x'(T)]^2}{N_0 T} \right\} \right) + z'(T) \cdot \text{erf} \left[ \frac{\sqrt{2}z'(T)}{\sqrt{N_0 T}} \right] \\ &\quad - x'(T) \cdot \text{erf} \left[ \frac{\sqrt{2}x'(T)}{\sqrt{N_0 T}} \right] \end{aligned} \quad (47)$$

After substitution for  $x'(T)$  and  $z'(T)$  from Eqs. (37) and (38),

$$\begin{aligned} \overline{\Delta(t)} &= \frac{1}{2} \sqrt{\frac{N_0 T}{\pi}} \left\{ \exp \left[ \frac{-8A^2 \left( \frac{T}{3} + 2\tau \right)^2 \cos^2(\phi)}{\pi^2 N_0 T} \right] \right. \\ &\quad \left. - \exp \left[ \frac{-8A^2 \left( \frac{T}{3} - 2\tau \right)^2 \cos^2(\phi)}{\pi^2 N_0 T} \right] \right\} + \frac{2\sqrt{2}A}{\pi} \\ &\quad \times \left\{ \left( \frac{T}{3} + 2\tau \right) \cos(\phi) \text{erf} \left[ \frac{4A \left( \frac{T}{3} + 2\tau \right) \cos(\phi)}{\pi \sqrt{N_0 T}} \right] \right. \\ &\quad \left. - \left( \frac{T}{3} - 2\tau \right) \cos(\phi) \text{erf} \left[ \frac{4A \left( \frac{T}{3} - 2\tau \right) \cos(\phi)}{\pi \sqrt{N_0 T}} \right] \right\} \end{aligned} \quad (48)$$

Equation (48) yields the expected result:

$$\begin{aligned} \overline{\Delta(t)} &= 0 & \text{when } \tau = 0 \\ \overline{\Delta(t)} &= 0 & \text{when } N_0 = 0 \end{aligned}$$

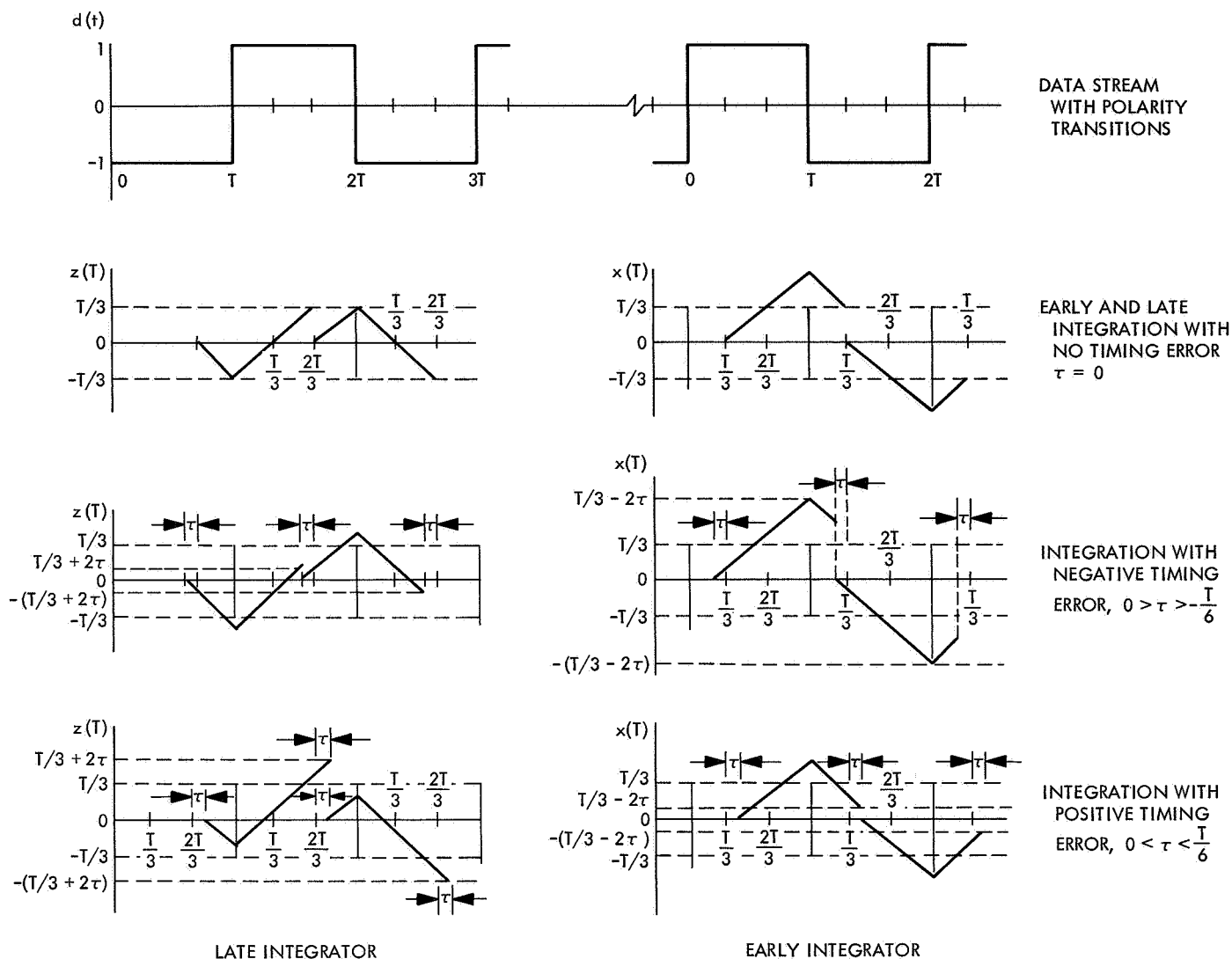


**Fig. 7. Bit timing loop: integrator output showing the effect of bit timing error**

After simplifying Eq. (48), with the substitutions:

$$\alpha = \left( \frac{T}{3} + 2\tau \right)$$

$$\beta = \left( \frac{T}{3} - 2\tau \right)$$

and if we let  $R = ST/N_0$  and  $r = 4\sqrt{R}/\pi T$  where  $S =$  signal amplitude  $= A^2$  and assume the subcarrier tracking loop is in lock ( $\phi \approx 0$ ) and ( $\tau \leq T/6$ ), then,

$$\begin{aligned} \overline{\Delta(t)} = & \frac{2A}{\pi\sqrt{\pi}r} \left[ \exp\left(-\frac{\alpha^2 r^2}{2}\right) - \exp\left(-\frac{\beta^2 r^2}{2}\right) \right] \\ & + \frac{2\sqrt{2}A}{\pi} [\alpha \cdot \text{erf}(\alpha r) - \beta \cdot \text{erf}(\beta r)] \end{aligned} \quad (49)$$

Equation (49) has been evaluated for several values of  $R$ . The result (Fig. 8) shows that the mean timing error is approximately linear over the range  $0 \leq \tau \leq T/12$  for  $[-4\text{dB} \leq R \leq 8\text{dB}]$ . Over this linear region, Eq. (49) reduces to

$$\overline{\Delta(t)} = \frac{2A}{\pi} \tau [0.91 + (0.12)(R)] \quad (50)$$

when the value for  $R$  is expressed in dB. Thus, the mean timing error is a function of both the timing offset and the signal-to-noise ratio.

A computed value of  $\Delta$  at some time  $t$  (where  $t$  is an integer number of bit periods) may differ from  $\overline{\Delta(t)}$  by an error,  $e$ , caused by noise and bit timing error.

$$\Delta(t) = \overline{\Delta(t)} + e_t \quad (51)$$

If  $k$  is defined as the slope of Eq. (49), then,

$$\Delta(t) = k\tau + e_t \quad (52)$$

The bit timing loop is locked in a manner analogous to the locking of the subcarrier tracking loop by changing the bit timing according to the previous bit error signal,

$$\tau_{t+1} = \tau_t - b\Delta(t) \quad (53)$$

where

$$b = K_a \cdot K_\tau$$

$K_a$  = multiplier constant

$K_\tau$  = VCO gain constant

In the absence of noise, Eqs. (52) and (53) combine to yield the transient response of the loop:

$$\tau_t = (1 - bk)^n \tau_0 \quad (54)$$

where

$\tau_0$  = initial bit timing error

$n$  = number of elapsed bit periods =  $t/T$

Combine Eqs. (51) and (54) for the variance of the bit timing loop  $\sigma_\tau^2$

$$\sigma_\tau^2 = \frac{bk}{2 - bk} \left( \frac{\sigma_\Delta^2}{k^2} \right) \quad (55)$$

where, by definition,

$$\sigma_\Delta^2 = \overline{\Delta^2(t)} - \overline{\Delta(t)}^2 \quad (56)$$

The next step is to determine  $\overline{\Delta^2(t)}$ . By squaring Eq. (39), we have

$$\overline{\Delta^2(t)} = \left\{ \begin{array}{l} \left\{ \begin{array}{l} [z(T) + n_4(t)]^2 + [x(T) + n_3(t)]^2 \\ -2 | [z(T) + n_4(t)] [x(T) + n_3(t)] | \end{array} \right\} \text{ with transition} \\ \text{probability} = 1/2 \end{array} \right\} \quad (57)$$

$$\left\{ \begin{array}{l} \left\{ \begin{array}{l} [z'(T) + n_4(t)]^2 + [x'(T) + n_3(t)]^2 \\ -2 | [z'(T) + n_4(t)] [x'(T) + n_3(t)] | \end{array} \right\} \text{ with transition} \\ \text{probability} = 1/2 \end{array} \right\}$$

After substitution,

$$\overline{\Delta^2(t)} = \frac{1}{2} [\overline{\epsilon_1^2} + \overline{\epsilon_2^2} - 2 |\overline{\epsilon_1 \epsilon_2}|] + \frac{1}{2} [\overline{(\epsilon'_1)^2} + \overline{(\epsilon'_2)^2} - 2 |\overline{\epsilon'_1 \epsilon'_2}|] \quad (58)$$

where

$$\epsilon_1 = z(T) + n_4(t)$$

$$\epsilon_2 = x(T) + n_3(t)$$

$$\epsilon'_1 = z'(T) + n_4(t)$$

$$\epsilon'_2 = x'(T) + n_3(t)$$

$\epsilon_1, \epsilon_2, \epsilon'_1, \epsilon'_2$  are gaussian random variables with

$$\overline{\epsilon_1} = z(T)$$

$$\overline{\epsilon_2} = x(T)$$

$$\overline{\epsilon'_1} = z'(T)$$

$$\overline{\epsilon'_2} = x'(T)$$

$$\sigma^2 \epsilon_1 = \sigma^2 \epsilon'_1 = \frac{N_0 T}{2} = \sigma^2$$

$$\sigma^2 \epsilon_2 = \sigma^2 \epsilon'_2 = \frac{N_0 T}{2} = \sigma^2 \quad (59)$$

The average  $|\overline{\epsilon_1 \epsilon_2}|$  is defined as

$$|\overline{\epsilon_1 \epsilon_2}| = \int_{-\infty}^{\infty} \int_{-\infty}^{\infty} |\epsilon_1 \epsilon_2| p(\epsilon_1, \epsilon_2) d\epsilon_1 d\epsilon_2 \quad (60)$$

The joint probability density function  $p(\epsilon_1, \epsilon_2)$  is

$$p(\epsilon_1, \epsilon_2) = \frac{1}{\sqrt{2\pi(1-\rho^2)}} \exp \frac{-\{[\epsilon_1 - z(T)]^2 - 2\rho[\epsilon_1 - z(T)][\epsilon_2 - x(T)] + [\epsilon_2 - x(T)]^2\}}{2\sigma^2(1-\rho^2)} \quad (61)$$

where  $\rho$  is the correlation coefficient, which we will define as

$$\rho = \frac{\overline{\epsilon_1 \epsilon_2} - \bar{\epsilon}_1 \bar{\epsilon}_2}{\sigma_{\epsilon_1} \sigma_{\epsilon_2}} \quad (62)$$

Upon expanding the numerator, we note that  $\epsilon_1$  and  $\epsilon_2$  are correlated only during the  $2T/3$  overlap in the bit timing loop integrations and are equal to each other during this time. During the  $2T/3$  overlap period,

$$\overline{\epsilon_1 \epsilon_2} - \bar{\epsilon}_1 \bar{\epsilon}_2 = \frac{2}{3} \sigma^2 \quad (63)$$

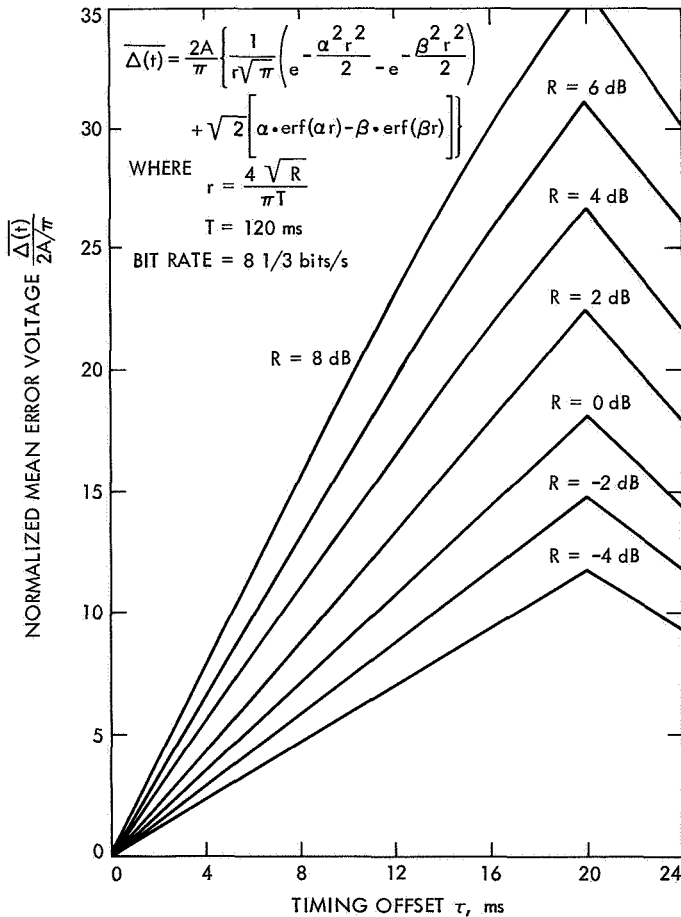


Fig. 8. Bit timing loop: average bit timing loop error voltage

and during the  $T/3$  nonoverlap period,

$$\bar{\epsilon}_1 \bar{\epsilon}_2 - \bar{\epsilon}_1 \bar{\epsilon}_2 = 0 \quad (64)$$

Thus,

$$\rho = \frac{2}{3} \quad (64)$$

Returning to Eq. (60),

$$\begin{aligned} |\overline{\epsilon_1 \epsilon_2}| &= \int_0^\infty \int_0^\infty \epsilon_1 \epsilon_2 p(\epsilon_1, \epsilon_2) d\epsilon_1 d\epsilon_2 \\ &\quad - \int_{-\infty}^0 \int_0^\infty \epsilon_1 \epsilon_2 p(\epsilon_1, \epsilon_2) d\epsilon_1 d\epsilon_2 \\ &\quad - \int_0^\infty \int_{-\infty}^0 \epsilon_1 \epsilon_2 p(\epsilon_1, \epsilon_2) d\epsilon_1 d\epsilon_2 \\ &\quad + \int_{-\infty}^0 \int_{-\infty}^0 \epsilon_1 \epsilon_2 p(\epsilon_1, \epsilon_2) d\epsilon_1 d\epsilon_2 \end{aligned} \quad (65)$$

After evaluating Eq. (65) by following an approach used by Stiffler (Ref. 9), we obtain the result:

$$\begin{aligned} |\overline{\epsilon_1 \epsilon_2}| &= \frac{2\sqrt{1-\rho^2}}{\sqrt{2\pi}} \int_0^\infty \left( y \exp - \left[ \frac{y^2 + z^2(T)}{2\sigma^2} \right] \right. \\ &\quad \times \cosh \left[ \frac{z(T)y}{\sigma^2} \right] \left. \left\{ \sqrt{\frac{2}{\pi}} \exp \left[ \frac{-x^2(T)}{2\sigma^2(1-\rho^2)} \right] \right. \right. \\ &\quad \left. \left. + \frac{\rho y}{\sigma \sqrt{1-\rho^2}} \operatorname{erf} \left[ \frac{\rho y}{\sqrt{2(1-\rho^2)}\sigma} \right] \right\} \right) dy \end{aligned} \quad (66)$$

In a similar manner, we can determine  $|\overline{\epsilon'_1 \epsilon'_2}|$ . In fact, it readily follows from Eq. (66):

$$\begin{aligned} |\overline{\epsilon'_1 \epsilon'_2}| &= \frac{2\sqrt{1-\rho^2}}{\sqrt{2\pi}} \int_0^\infty \left( y \exp - \left\{ \frac{y^2 + [z'(T)]^2}{2\sigma^2} \right\} \right. \\ &\quad \times \cosh \left[ \frac{z'(T) \cdot y}{\sigma^2} \right] \left\{ \sqrt{\frac{2}{\pi}} \exp \left\{ \frac{-[x'(T)]^2}{2\sigma^2(1-\rho^2)} \right\} \right. \\ &\quad \left. \left. + \frac{\rho y}{\sigma \sqrt{1-\rho^2}} \operatorname{erf} \left[ \frac{\rho y}{\sqrt{2(1-\rho^2)}\sigma} \right] \right\} \right) dy \end{aligned} \quad (67)$$

Finally, we have a solution for Eq. (58) and thus an expression for the bit timing loop variance:

$$\sigma_{\tau}^2 = \frac{bk}{2 - bk} \left( \frac{\frac{1}{2} \{x^2(T) + z^2(T) + [x'(T)]^2 + [z'(T)]^2\} - |\overline{\epsilon_1 \epsilon_2}| - |\overline{\epsilon'_1 \epsilon'_2}| - \overline{\Delta(T)^2} + N_o T}{k^2} \right) \quad (68)$$

### E. Digitization of the VCO

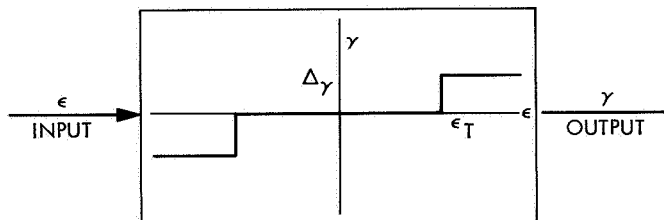
In the continuous system, the VCO output  $\gamma$  is a linear function of the input error signal  $\epsilon$ .

$$\gamma = K_{VCO} \cdot \epsilon \quad (69)$$

where  $K_{VCO}$  is the VCO gain constant (slope) defined as

$$K_{VCO} = \frac{\text{incremental output}}{\text{incremental input}} = \frac{\Delta\gamma}{\Delta\epsilon}$$

Consider now a nonlinear device, such as the digital mechanization of the VCO shown in Sketch A. The output signal  $\gamma$  is zero until the error voltage exceeds threshold  $\epsilon_T$ . At that time the VCO output is a step response with height  $\Delta\gamma$ .



Sketch A. Digital VCO

We want to find the average VCO response. Assume the input  $\epsilon$  is a gaussian random process, with mean =  $\bar{\epsilon}$  and variance =  $\sigma_{\epsilon}^2$ . The average VCO output  $\bar{\gamma}$  is

$$\begin{aligned} \bar{\gamma} &= \Delta\gamma [P(\bar{\epsilon} < -\epsilon_T) + 0 \cdot P(-\bar{\epsilon}_T < \epsilon < \epsilon_T) + \Delta\gamma P(\bar{\epsilon} > \epsilon_T)] \\ &= \Delta\gamma \left[ \int_{\epsilon_T}^{\infty} N(\bar{\epsilon}, \sigma_{\epsilon}) dx - \int_{-\infty}^{\epsilon_T} N(\bar{\epsilon}, \sigma_{\epsilon}) dx \right] \quad (70) \\ &= \Delta\gamma \left[ \text{erfc} \left( \frac{\epsilon_T - \bar{\epsilon}}{\sigma_{\epsilon}} \right) - \text{erfc} \left( \frac{\epsilon_T + \bar{\epsilon}}{\sigma_{\epsilon}} \right) \right] \end{aligned}$$

Upon using the definition of the error function, we have

$$\bar{\gamma} = \Delta\gamma \left[ \text{erf} \left( \frac{\epsilon_T + \bar{\epsilon}}{\sigma_{\epsilon}} \right) - \text{erf} \left( \frac{\epsilon_T - \bar{\epsilon}}{\sigma_{\epsilon}} \right) \right] \quad (71)$$

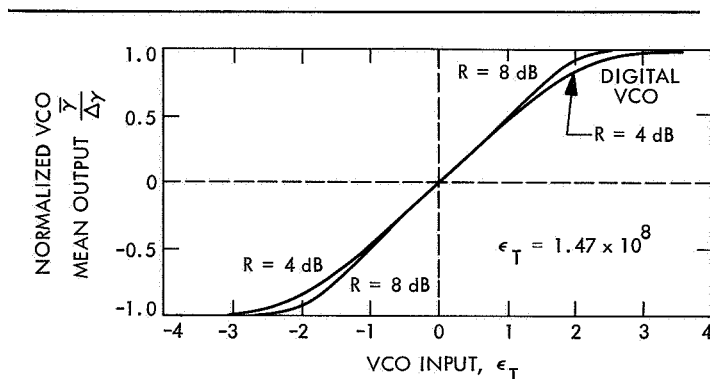


Fig. 9. Mean output of a digital voltage controlled oscillator

Equation (71) is shown in Fig. 9. Equation (71) is applicable to the VCOs in the bit timing loop and subcarrier tracking loop when  $\bar{\epsilon}$  is replaced by the appropriate  $u(T)$ ,  $w'(T)$ ,  $w(T)$ ,  $w'(T)$ ,  $x(T)$ ,  $x'(T)$ ,  $z(T)$ , or  $z'(T)$ .

This degradation of the loop VCO constant caused by the nonlinearity of the digital VCO will be an important factor in the selection of the bit timing and subcarrier tracking phase loop threshold.

### F. Probability of Error

The probability of error (or bit error rate) is a convenient means of comparing the performance of telemetry demodulators. In this section, we will rely upon the linear analysis by Lindsey (Ref. 12) for the uncoded coherent PSK sine wave subcarrier channel. Considering only the phase jitter and disregarding the bit timing jitter, Lindsey demonstrated that the probability of error,  $P_E$ , for the sine wave subcarrier tracking loop is

$$P_E =$$

$$\frac{1}{2} \left[ 1 - \sqrt{\frac{4R}{\pi}} \exp\left(-\frac{R}{2}\right) \sum_{k=0}^{\infty} (-1)^k \epsilon_k b_{2k+1} \frac{I_k\left(\frac{R}{2}\right)}{(1-4k^2)} \right] \quad (72)$$

Using Lindsey's notation,

$$b_{ak+1} = \frac{I_k(\hat{\delta}R)}{I_0(\hat{\delta}R)}$$

$$R = \frac{ST}{N_0}$$

$$\hat{\delta} = \frac{2\mathcal{R}}{B_L \left(1 + \left(\frac{2}{R}\right)\right)}$$

$$\mathcal{R} = \frac{1}{T}$$

Digress for a moment to consider the bandwidth of the Costas loop,  $B_L$ . The overall loop transfer function  $L(s)$  is

$$L(s) = \frac{1}{\alpha s + 1} \quad (73)$$

where  $\alpha$  is the time constant of the loop. The response of the loop from Eq. (29) is

$$\frac{\phi_t}{\phi_0} = (1 - ch)^{t/T} = e^{-t/\alpha} \quad (74)$$

where  $t = nT$

Thus,

$$\alpha = \frac{-T}{\ln(1 - ch)} \quad (75)$$

From the linear phase locked loop theory (Ref. 13) for the first-order loop,

$$B_L = \frac{1}{2\pi f} \int_{-j\infty}^{j\infty} |L(s)|^2 ds \quad (76)$$

$$= \frac{1}{2\alpha}$$

Finally,

$$B_L = -\frac{\ln(1 - ch)}{2T} \quad (77)$$

Since Lindsey's result is for a system with a sine wave reference in the Costas loop, Eq. (72) will be degraded 0.9 dB when used with a square wave Costas loop reference.

### III. Software Description

#### A. The Computer and ADC

The digital demodulator is a computer program, written in SDS symbol language for the SDS 920 computer.

The program performs three major functions: (1) the acquisition of phase lock with the data subcarrier, (2) the acquisition of bit timing lock with the incoming data stream, and (3) the acquisition of frame and word synchronization. The computer then outputs data, bit sync, and word sync in a form suitable for processing in the decommutation program.

The ADC converts the analog signal input from the receiver to digital values for input to the computer. The ADC format is 11 bits plus sign. It receives its digitize commands at a 1-KHz rate from the computer millisecond clock.

#### B. The Subcarrier Tracking Loop

The digital mechanization of the subcarrier tracking loop is shown in Fig. 10. The integrators are replaced by their digital equivalent summing networks. Also, the phase error  $\delta(t)$  is summed over 4 calculations before it is compared to the phase threshold. The program samples the incoming data signal every 54 deg and multiplies this value by the square wave VCO output. The loop then integrates, multiplies, and adjusts the square wave phase as necessary to achieve and maintain phase lock.

#### C. Bit Timing Loop

The theoretical integrators in the bit timing loop (Fig. 11) are also replaced by discrete summing devices. The difference of the early and late timing sums for 4 bit times is stored before it is compared with the bit position error threshold. If the error exceeds threshold, the bit timing is changed by  $T/120$ . The excess over the threshold is then saved for the next threshold comparison.

#### D. Frame Sync and Word Sync

Frame synchronization is performed by correlating the incoming data stream with the known *Mariner* mode II (420 frame) in which the first 7 bits of a frame are *one* bits (engineering sync) and the 141st thru 155th bits are a 15-bit PN code (science sync). Once frame and word sync have been achieved, the program outputs both word sync and bit sync to the decommutation program.

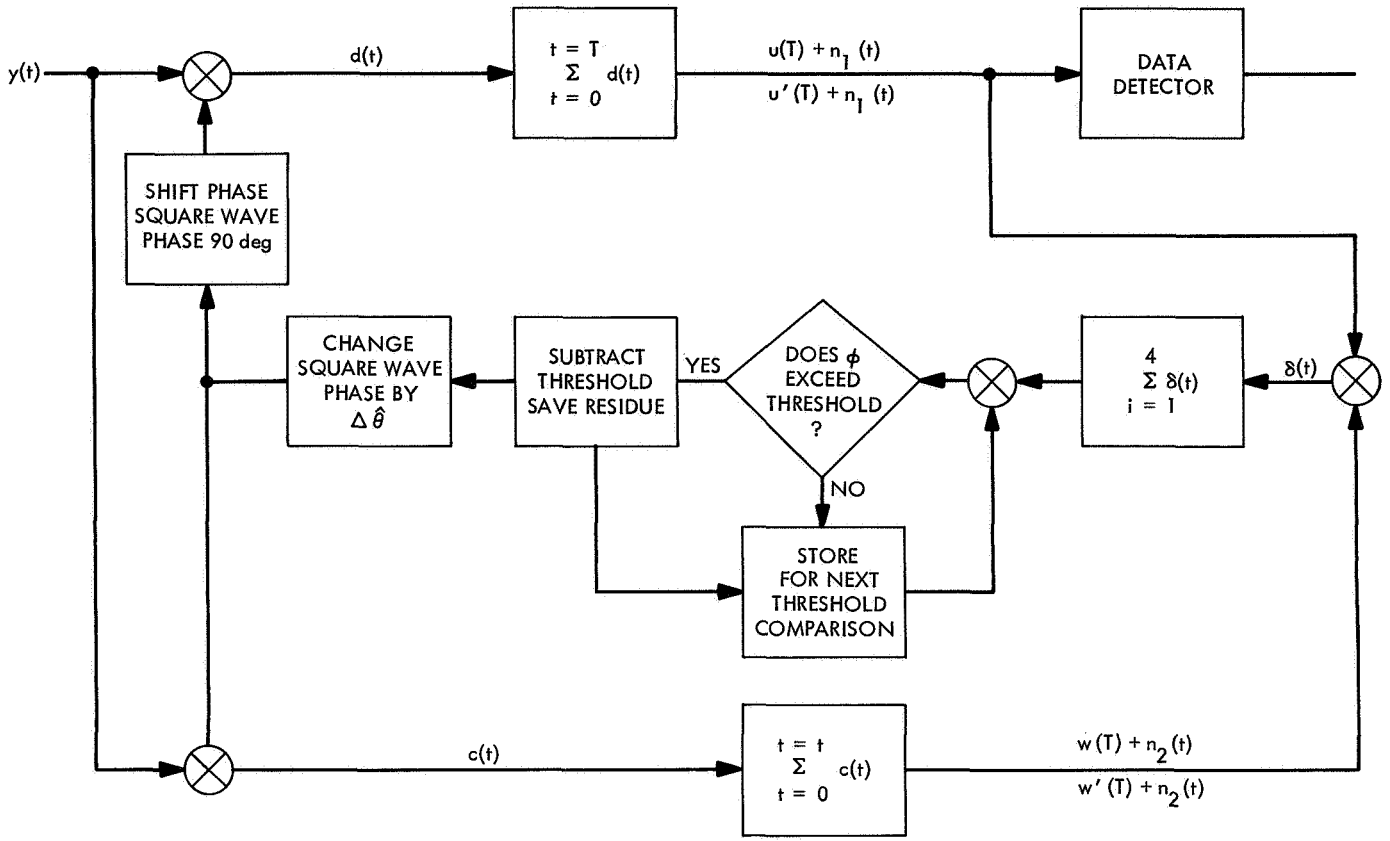


Fig. 10. Computer algorithm for the subcarrier tracking loop

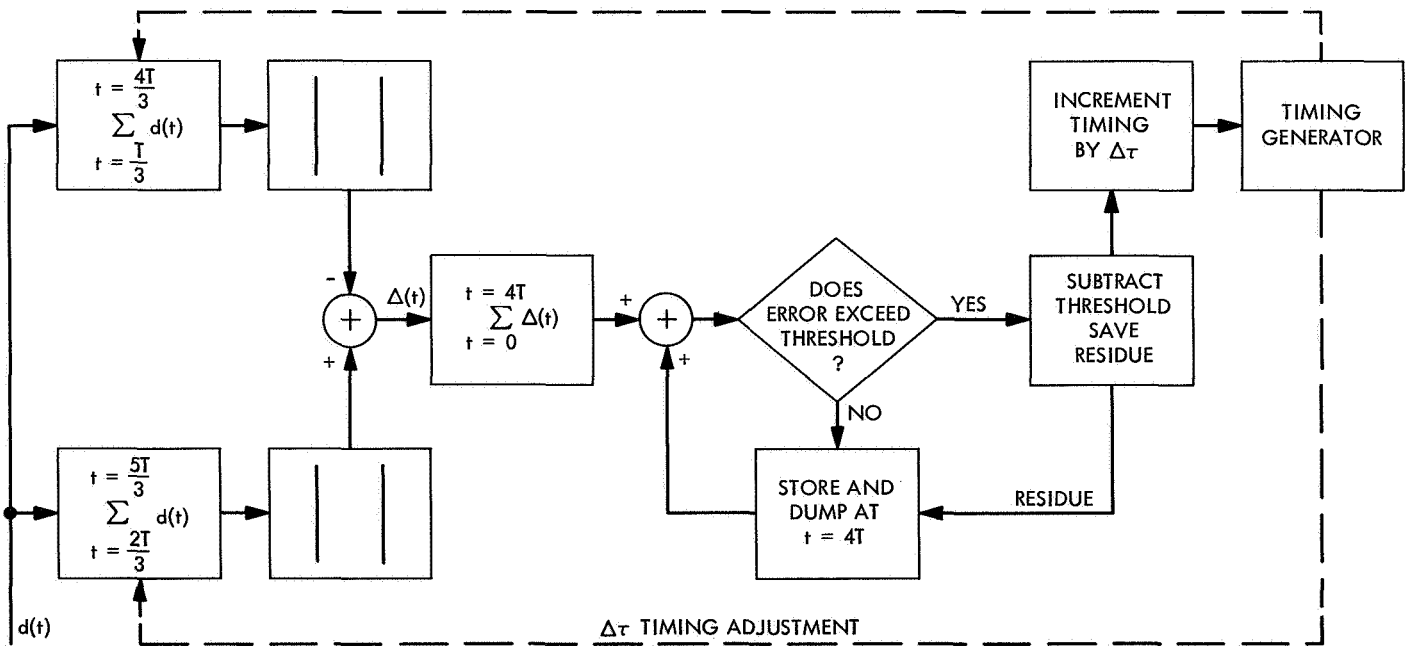


Fig. 11. Computer algorithm for the bit timing loop

### E. Computer Scaling

The ADC converts an input voltage to a binary number. For a 10-V input, the ADC outputs the number  $(2^{11} - 1)$  or 2047. The ADC is linear and its scale factor,  $K_{\text{ADC}}$ , is

$$K_{\text{ADC}} = 204.7 \text{ bits/V}$$

The computer timing and ADC sampling are derived from the millisecond clock. This means that all incoming frequencies are converted to samples per second according to the computer timing ratio  $K_T$ .

$$K_T = 1000 \text{ samples/s}$$

### F. Variable Loop Parameters

The program accepts the following loop parameters from the typewriter:

- (1)  $4f_s$  sample rate =  $0.36F = (1 - \Delta f/f)$  (150) (0.36)  
where:

$$\Delta f = \text{doppler frequency offset from nominal}$$

$$f = \text{nominal downlink subcarrier frequency}$$

- (2) Subcarrier tracking loop error threshold =  $\delta_T$   
(3) Subcarrier tracking loop VCO step response =  $\Delta \hat{\theta}$   
(4) Bit timing loop error threshold =  $\Delta_T$   
(5) Bit timing loop VCO step response =  $\Delta \tau$

## IV. System Design

The operation of the digital demodulator depends upon the selection of the proper loop parameters.

### A. Subcarrier Tracking Loop

The product of the composite loop gain  $c$  and the slope  $h$  of the loop error voltage  $\delta(t)$  determines the response of the subcarrier tracking loop in the absence of noise. If  $ch = 1$ , the loop is critically damped and it removes the initial phase error in one sample. If  $ch < 1$ , the loop is underdamped, which is the region of desired operation.

If we assume that the multiplier gain  $K_m$  is unity, then the phase loop VCO gain constant  $K_o$  is

$$K_o = \frac{\Delta \hat{\theta}}{\delta_T}$$

Once the product  $ch$  has been specified, the VCO gain constant is then determined by selecting  $\Delta \hat{\theta}$  and  $\delta_T$  sub-

ject to operation in the linear region of Eq. (71) over the expected signal-to-noise ratio.

### B. Bit Timing Loop

The product of the loop gain  $b$  and the slope of the loop timing error  $h$  is specified in a similar manner for the bit timing loop. The loop gain, which was previously defined as

$$b = K_T \cdot K_u$$

is equal to the VCO constant when the multiplier gain  $K_u$  is unity. The VCO outputs  $\Delta \tau$  when the timing error exceeds  $\Delta_T$ . The step response of the VCO is then

$$K_\tau = \frac{\Delta \tau}{\Delta T}$$

The selection of  $\Delta_T$  and  $\Delta \tau$  (once  $b \cdot h$  has been specified) is also subject to the constraint that the operation should be in the linear region of Eq. (71).

### C. Performance

The digital demodulator was operated successfully during the *Mariner IV* reacquisition in September 1967. The following parameters were determined theoretically and used in the computer program.

$$\delta_T = 3.53 \times 10^{-3} \text{ (V-s)}^2$$

$$\Delta \hat{\theta} = 0.0698 \text{ (Rad)}$$

$$\Delta_T = 0.547 \text{ (V-s)}$$

$$\Delta \tau = 10^{-3} \text{ (s)}$$

After calculating the mean and variance of  $\phi$  and determining the average subcarrier tracking loop VCO output, notice that for the signal-to-noise ratios of interest ( $R = 2$  to 8 dB) and for the phase threshold that was selected, the average VCO output is about  $\Delta \hat{\theta}/2$  or 0.0349 radians when  $\delta(T)$  exceeds  $\delta_T$ . The phase loop constant  $ch$  is approximately 0.1075. The subcarrier tracking loop phase error is summed over 4 bit times. If this sum exceeds 18 deg (or 4.5 deg/bit) the average phase is adjusted by 2 deg.

In the bit timing loop the timing error is summed over 4 bit periods. As shown in Fig. 8 the average timing error is a function of the parameter  $R$ . At  $R = 2$ , the error accumulates to 19.3 ms before a shift of 1 ms is made. At  $R = 8$  dB, a shift of 1 ms is made when the timing error



reaches 11.9 ms. The average timing shift differs from the instantaneous due to the nonlinear VCO.

The performance of the digital demodulator was verified experimentally by counting the errors in demodulating a known data stream. The results of this test are shown in Fig. 12. Over the region of interest the experimental  $P_E$  agreed with the theoretical  $P_E$ .

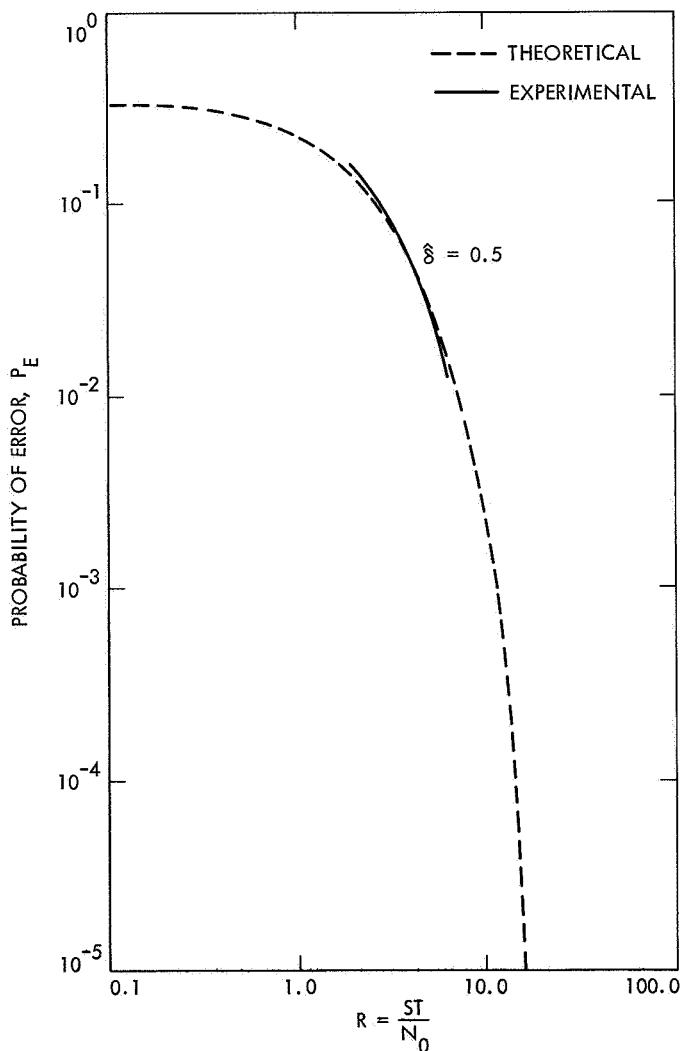


Fig. 12. Digital demodulator error probability

## V. Summary and Recommendations

The *Mariner* digital demodulator was an experimental effort to develop a computer-aided demodulator that would operate in real time with a flight project and have the design capability to tolerate relatively slow computation time such as in the SPS 920 computer. The effort was very successful. The digital demodulator was installed at DSN stations 11, 12, and 51, giving nearly con-

tinuous telemetry coverage of the *Mariner IV* and *V* spacecraft during periods of low received signal strength.

While noting the success of the effort, mention should be made of the compromises which were made in the design.

### A. Square Wave VCO Output Waveform

The input to the Digital Demodulator program is the first harmonic of the *Mariner 1967* telemetry data signal. Optimum demodulation would be accomplished by mixing the received data signal with a sine wave subcarrier reference in the Costas loop. When a square wave reference is used, this results in a 0.9-dB power loss. The square wave reference was used because a sine wave VCO output would require the storage of a sine table and the subsequent table lookup time in the computer.

### B. T/3 Bit Timing

In the bit timing loop, the bit stream was sampled  $T/3$  before a transition and  $T/3$  after the transition. This left an overlap of  $2T/3$  during which the noise was correlated. For  $T/4$  early-late timing, the noise would be correlated for  $T/2$  s, thus reducing the contribution of the noise to the bit timing jitter. The  $T/3$  early-late scheme was chosen since the bit time is evenly divisible by the period of the data subcarrier, allowing the program to be written in single precision notation. A fractional division would necessitate double precision arithmetic with the subsequent increase in computer time.

### C. The Difference of Absolute Values

The outputs of the early and late integrators are differenced in magnitude in this digital demodulator. This operation was selected because of the saving in operation time in taking the absolute value of a number as compared with squaring in the computer. The expression for the mean and variance for the difference of squares however is quite simple compared with the difference of absolute values. The mean error for the absolute value case is a function of the input signal-to-noise ratio. Stiffler (Ref. 9) demonstrated that for the difference of squares case the mean error is independent of  $R$ . In the former case, then, the parameter  $R$  must be supplied to the computer program if a constant bit error threshold is to be used for all  $R$ .

### D. Storage of the Error Voltages for Four Bit Times

In both the loops, the loop error is summed over four bit times. This scheme was proposed in an attempt to

decrease the noise contribution to the loop jitter. This is true if the sum is normalized over the number of bits,  $n$ . Since the noise jitter for  $n$  bit times,

$$\sigma = \left( \frac{N_0 n T}{a} \right)^{1/2}$$

increases as a function of  $(n)^{1/2}$ . The noise jitter per bit is then  $[(n)^{1/2}/n] \sigma$ . However, the quantization of the VCO as a nonlinear function must be considered. Summing the loop error over  $n$  bits results in a higher threshold. This higher threshold can be avoided by normalizing the sum over the number bit periods.

## References

1. *Mariner C Data Demodulator Study Program, Final Engineering Report*, 7-801002. Texas Instruments, Inc., Dallas, Tex., Jan. 15, 1968.
2. Lindsey, W. C., "Determination of Modulation Indexes and Design of Two-Channel Coherent Communication Systems," *IEEE Transactions on Communication Technology*, Vol. Com-15, No. 2, pp. 229-237, April 1967.
3. Van Trees, H., *Optimum Power Division in Coherent Communication Systems*, Technical Report No. 301. Massachusetts Institute of Technology, Lincoln Laboratory, Lexington, Mass., Feb. 1963.
4. Layland, J. W., *Signal Design for Communication with Timing Uncertainties*, Ph.D. thesis. Carnegie Institute of Technology, Pittsburgh, Pa., June 1965.
5. Stiffler, J. J., "On the Allocation of Power in a Synchronous Binary PSK Communication System," *Proceedings of the 1964 National Telemetry Conference*, June 2-4, 1964.
6. Costas, J. P., "Synchronous Communication," *Proceedings of the IRE*, Vol. 44, pp. 1713-1718, Dec. 1956.
7. Stiffler, J. J., "A Comparison of Several Methods of Subcarrier Tracking," *Space Programs Summary 37-37*, Vol. IV, pp. 268-275. Jet Propulsion Laboratory, Pasadena, Calif., Feb. 28, 1966.
8. Lindsey, W. C., "Subcarrier Tracking Methods and Communication System Design," *Space Programs Summary 37-44*, Vol. IV, pp. 271-281. Jet Propulsion Laboratory, Pasadena, Calif., April 30, 1967.
9. Stiffler, J. J., "On Suboptimum Binary Decisions," *Space Programs Summary 37-29*, Vol. IV, pp. 285-286. Jet Propulsion Laboratory, Pasadena, Calif., Oct. 31, 1964.
10. Davenport, W. B. Jr., and Root, W. L., *Random Signals and Noise*, pp. 160. McGraw-Hill Book Co., Inc., New York, N.Y., 1958.
11. Papoulis, A., *Probability, Random Variables, and Stochastic Processes*, pp. 502-505, McGraw-Hill Book Co., Inc., New York, N.Y., 1965.
12. Lindsey, W. C., "Phase-Shift-Keyed Signal Detection with Noisy Reference Signals," *IEEE Transactions on Aerospace and Electronic Systems*, Vol. AES-2, No. 4, pp. 393-401, July 1966.
13. Tausworthe, R. C., *Theory and Practical Design of Phase-Locked Receivers*, Technical Report 32-819, Vol. 1. Jet Propulsion Laboratory, Pasadena, Calif., Feb. 15, 1966.